Published in The Plant Journal, Vol. 77, Issue 2, 2014, p. 269–283
which should be used for any reference to this work

ABC1K1/PGR6 kinase: a regulatory link between photosynthetic activity and chloroplast metabolism

Jacopo Martinis[1], Gaétan Glauser[2], Sergiu Valimareanu[1], Michaela Stettler[3], Samuel C. Zeeman[3], Hiroshi Yamamoto[4], Toshiharu Shikanai[4] and Felix Kessler[1,*]

[1]*Laboratory of Plant Physiology, University of Neuchâtel, 2000 Neuchâtel, Switzerland,*
[2]*Chemical Analytical Service of the Swiss Plant Science Web, University of Neuchâtel, 2000 Neuchâtel, Switzerland,*
[3]*The Institute of Agricultural Sciences, ETH Zurich, Universitätstrasse 2, CH-8092 Zurich, Switzerland, and*
[4]*Department of Botany, Graduate School of Science, Kyoto University, Sakyo-ku, Kyoto 606-8502, Japan*

*For correspondence (e-mail felix.kessler@unine.ch).

SUMMARY

Arabidopsis proton gradient regulation (*pgr*) mutants have high chlorophyll fluorescence and reduced non-photochemical quenching (NPQ) caused by defects in photosynthetic electron transport. Here, we identify PGR6 as the chloroplast lipid droplet (plastoglobule, PG) kinase ABC1K1 (activity of *bc1* complex kinase 1). The members of the ABC1/ADCK/UbiB family of atypical kinases regulate ubiquinone synthesis in bacteria and mitochondria, and impact various metabolic pathways in plant chloroplasts. Here, we demonstrate that *abc1k1* has a unique photosynthetic and metabolic phenotype that is distinct from that of the *abc1k3* homolog. The *abc1k1/pgr6* single mutant is specifically deficient in the electron carrier plastoquinone, as well as in β–carotene and the xanthophyll lutein, and is defective in membrane antioxidant tocopherol metabolism. After 2 days of continuous high light stress, *abc1k1/pgr6* plants suffer extensive photosynthetic and metabolic perturbations, strongly affecting carbohydrate metabolism. Remarkably, however, the mutant acclimates to high light after 7 days together with a recovery of carotenoid levels and a drastic alteration in the starch-to-sucrose ratio. Moreover, ABC1K1 behaves as an active kinase and phosphorylates VTE1, a key enzyme of tocopherol (vitamin E) metabolism *in vitro*. Our results indicate that the ABC1K1 kinase constitutes a new type of regulatory link between photosynthetic activity and chloroplast metabolism.

Keywords: ABC1-like kinase, non-photochemical quenching, PGR6, photosynthesis, carotenoids, vitamin E, *Arabidopsis thaliana*.

INTRODUCTION

Photosynthesis is the single entry point for CO_2 into the biosphere and the food chain. To date, major questions exist regarding the regulatory links and coordination between photosynthetic light reactions and subsequent carbon fixation, as well as the subsequent allocation of fixed carbon to different pathways. Photosynthesis itself is a highly dynamic process quickly reacting to the changing light environment in nature. Non-photochemical quenching (NPQ) of chlorophyll fluorescence is a key mechanism for the thermal dissipation of excess light energy. The genetic screening for Arabidopsis mutants with reduced NPQ led to the discovery of Arabidopsis proton gradient regulator (*pgr*) mutants, which are defective in the regulation of photosynthetic electron transport and in the generation of the pH gradient across thylakoid membranes (Shikanai *et al.*, 1999). The molecular mechanisms affected in these mutants are different, but they all reduce quenching of chlorophyll fluorescence. Among these, the *pgr1* mutant has a miss-sense mutation in the Rieske Fe–S subunit of the cyt b_6f complex, the activity of which is hypersensitive to lumenal acidification at high light intensity (Munekage *et al.*, 2001; Jahns *et al.*, 2002). The *pgr5* mutant is defective in cyclic electron flow around photosystem I (PSI), which leads to reduced NPQ and the over-reduction of PSI (Munekage *et al.*, 2002). The *pgr6* mutant was originally isolated as CE11-8–1 (Columbia *gl1* accession 11–8–1; Shikanai *et al.*, 1999). Here, we demonstrate that *PGR6* is identical to the chloroplast ABC1-like kinase ABC1K1 (At4g31390). The family of ABC1/ADCK/UbiB (activity of *bc1* complex/ABC1 domain-containing kinase/ubiquinone biosynthesis protein B) atypical kinases is conserved from prokaryotes (Archaea and bacteria) to

eukaryotes (Lundquist *et al.*, 2012a). The biological roles of these kinases have been investigated in bacteria, yeast and human mitochondria, and in plant chloroplasts. The prototypical family member, *Saccharomyces cerevisiae* ABC1/Coq8 (coenzyme Q biosynthesis) is required for aerobic respiration at the level of the mitochondrial bc_1 complex (Poon *et al.*, 2000). *abc1* mutants lack ubiquinone (a member of the prenylquinone family) and are defective at the first monooxygenase step in its biosynthesis. Nevertheless, the data for ABC1 point to a regulatory role rather than an enzymatic function in biosynthesis. In yeast, the phosphorylation of Coq3, Coq5 and Coq7 of the ubiquinone pathway depends on ABC1/Coq8. The yeast *coq8* mutant is rescued by the human homolog ADCK3/CABC1, which also reinstates phosphorylation of several of the Coq proteins. This provides evidence for multiple kinase targets in the ubiquinone biosynthesis pathway (Xie *et al.*, 2011).

In Arabidopsis, six of eight ABC1-like kinases, including ABC1K1, are enriched in the plastoglobule (PG) proteome (Vidi *et al.*, 2006; Ytterberg *et al.*, 2006; Lundquist *et al.*, 2012b, 2013). PGs are lipid droplets inside plastids (Brehelin and Kessler, 2008), and participate in prenylquinone (tocopherols, phylloquinone and plastoquinone) as well as carotenoid metabolism and storage. PG hosts tocopherol cyclase (VTE1), a key enyzme in vitamin E synthesis and recycling (Kobayashi and DellaPenna, 2008; Szymanska and Kruk, 2010). VTE1 may be regulated by phosphorylation, as it has been identified in a large-scale comparative phosphoproteomics screen (Nakagami *et al.*, 2010). In conclusion, current knowledge suggests that the chloroplast ABC1-like homologs participate in the modulation of prenylquinone metabolism, similar to mitochondrial ABC1-like kinases in ubiquinone biosynthesis. In support of this hypothesis, evidence for the involvement of the PG kinase ABC1K3 in the regulation and phosphorylation of VTE1 activity has been found (Martinis *et al.*, 2013). Moreover, double-mutant analysis suggested that ABC1K1 and ABC1K3 may act in concerted fashion to phosphorylate and regulate VTE1 (Lundquist *et al.*, 2013). Beyond prenylquinone metabolism, a recent genome-wide co-expression analysis, in combination with experimentation, showed that PG ABC1-like kinases are involved in carotenoid biosynthesis, photoacclimation, plastid biogenesis and senescence, suggesting the existence of a much wider regulatory network affecting multiple metabolic pathways (Lundquist *et al.*, 2012b).

ABC1K1 is required to stabilize chlorophyll-binding proteins in photosynthetic complexes, and knock-down plants accumulate chlorophyll degradation products, have a lower anthocyanin content and are more sensitive to photooxidative stress under high light conditions (Yang *et al.*, 2012; Lundquist *et al.*, 2013). In addition to the unique *pgr* phenotype, our findings indicate that the *abc1k1/pgr6* mutation specifically and severely affects sugar metabolism. Prenylquinone and carotenoid metabolism may be regulated pleiotropically by both the ABC1K1 and ABC1K3 homologs. Considering the range of photosynthetic and metabolic alterations in the mutant *abc1k1*, ABC1K1 may act to integrate photosynthetic activity with adjacent metabolic pathways in chloroplasts.

RESULTS

Phenotype of the *abc1k1/pgr6* mutant

Moderate light intensity (150 μE m^{-2} sec^{-1}) affected the size and morphology of the *abc1k1/pgr6* mutant in young rosettes (up to 3 weeks old), but they later recovered to wild-type Col–0 (abbreviated as WT), although *abc1k1/pgr6* leaves were slightly thinner under all light conditions (Figure 1a,d). After a short exposure to continuous high light (HL, 500 μE m^{-2} sec^{-1}) treatment, *abc1k1/pgr6* suffered visible photodamage and had little or no anthocyanin as well as reduced chlorophyll content (Figure 1b,c,e), in agreement with previous observations (Yang *et al.*, 2012; Lundquist *et al.*, 2013). However, *abc1k1/pgr6* acclimated to prolonged HL treatment concurrently with a slight recovery of anthocyanin levels. Chloroplast ultrastructure was also affected in the *abc1k1/pgr6* mutant, expecially after HL treatment. In particular, very few starch granules were detected in chloroplasts from *abc1k1/pgr6* leaves, and the grana appeared less organized and puffy when compared with the WT (Figure 1f,g).

Photosynthetic activity is impaired in the *abc1k1/pgr6* mutant

In order to evaluate the photosensitivity of the *abc1k1/pgr6* mutant under light stress conditions, chlorophyll fluorescence measurements were carried out using a Mini-PAM device to determine photosynthetic parameters. At the same time, photosynthetic gas exchange was measured in order to determine the CO_2 assimilation rate in both WT and *abc1k1/pgr6*. A dramatic reduction in maximum PSII quantum efficiency (F_v/F_m) was observed in the *abc1k1/pgr6* mutant after a short exposure (1–2 days) to HL conditions. F_v/F_m = maximum quantum yield of Photosystem II, calculated as $(F_m\text{-}F_0)/Fm$, where F_0 and F_m are the minimal and maximal fluorescence, respectively. Strikingly, however, maximum PSII activity recovered to almost normal levels after prolonged HL treatment (Figure 2a). This was confirmed by the analysis of photosynthetic gas exchange in *abc1k1/pgr6*, showing a strong initial decrease in CO_2 assimilation and recovery to WT levels during 8 days of exposure to HL (Figure 2d). Consistent with the *pgr6* phenotype (Figure 2a–d), the electron transport rate (ETR) in *abc1k1/pgr6* was also affected in plants grown under moderate light intensities, and saturated at half the level of the WT (Figure 2b). NPQ was severely reduced, although *abc1k1/pgr6* still exhibited light intensity-dependent NPQ induction when grown under moderate light conditions

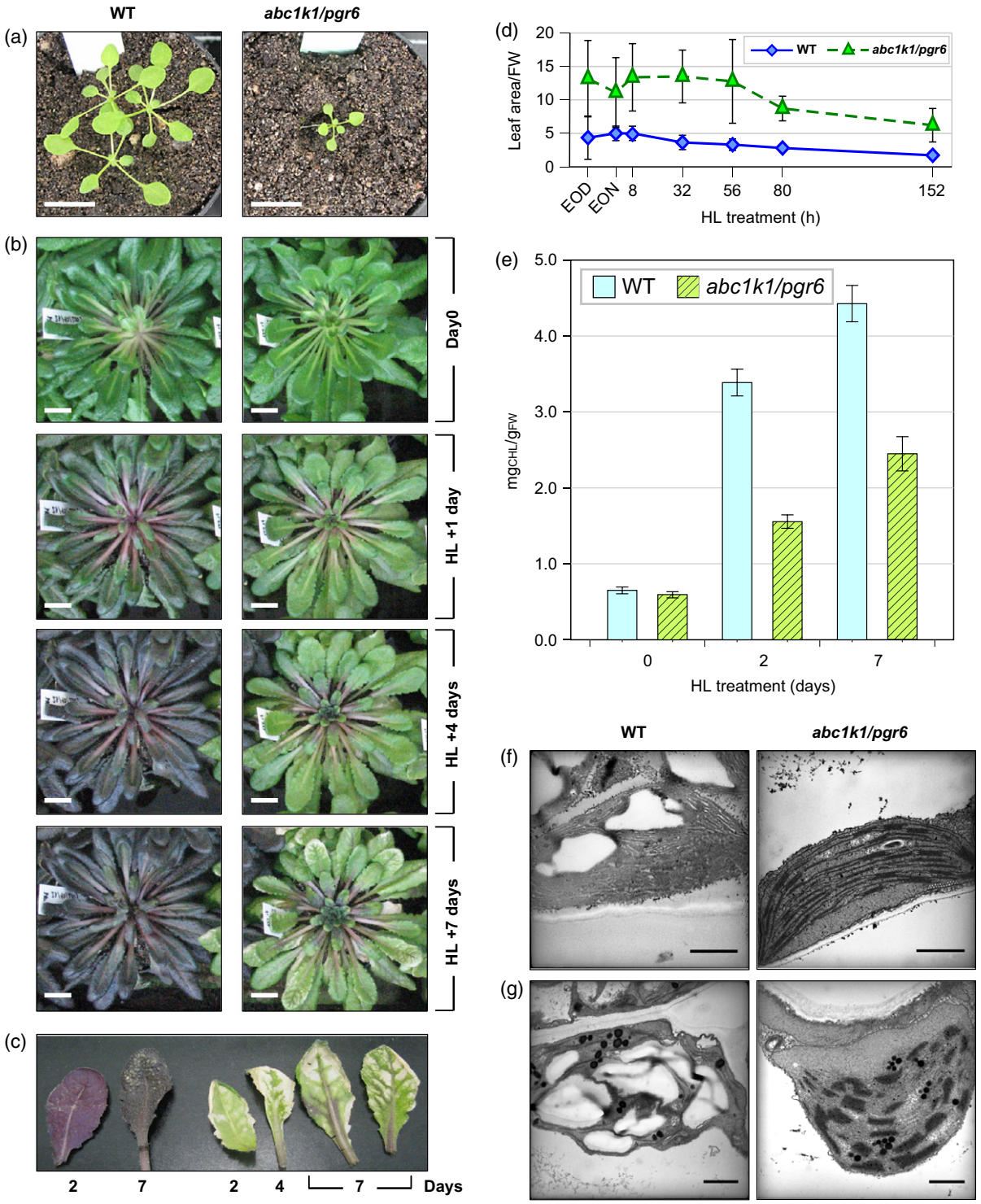

Figure 1. Phenotype of the *abc1k1/pgr6* single mutant and comparison with the *abc1k3* single mutant.
(a) Comparison of 3–week-old plants grown on soil under moderate light conditions (150 μE m^{-2} sec^{-1}).
(b) Total rosettes exposed to continuous high light (HL, 500 μE m^{-2} sec^{-1}) for the indicated number of days.
(c) Detail of leaves from plants exposed to continuous HL. Scale bars: 1 cm.
(d) Changes in leaf thickness. The leaf surface/fresh weight ratio (mm^2 mg^{-2}) was determined in leaves (n = 8) from WT and *abc1k1/pgr6* mutant plants.
(e) Changes in chlorophyll content in leaves (n = 3).
(f, g) Changes in chloroplast ultrastructure observed under HL treatment.
(f) Transmission electron micrographs of leaves exposed to moderate light intensity (150 μE m^{-2} sec^{-1}).
(g) Sections of leaves exposed to continuous HL (500 μE m^{-2} sec^{-1}) for 4 days. Scale bars: 1 μm.

(Figure 2e). After a short HL exposure, a pronounced drop in ETR (maximal after 48 h) and a lesser drop in NPQ was observed in the mutant (Figure 2c,f, respectively). However, ETR and NPQ in the mutant recovered to the original levels after 7 days of HL treatment (168 h), but did not reach those of the WT (Figure 2c,f). No overall increase of NPQ in *abc1k1/pgr6* was detected after prolonged HL treatment, as was the case in the WT (Figure 2e).

The *abc1k3* single mutant was analyzed in parallel, but did not show the *pgr* phenotype observed in the *abc1k1/pgr6* single mutant. *abc1k3* photosynthetic parameters and CO_2 assimilation were similar to the WT or only slightly lower (Figure 2), as previously reported (Martinis *et al.*, 2013). Moreover, the ETR defect was strongly enhanced in the *pgr1 pgr6* double mutant, which carries an additional point mutation in the Rieske subunit of the Cyt b_6f complex, making it hypersensitive to lumenal acidification under HL intensity in the *pgr1* single mutant (Munekage *et al.*, 2001; Jahns *et al.*, 2002). The *pgr1 pgr6* mutant showed a drastic reduction of ETR even at moderate light intensity, suggesting that the activity of the Cyt b_6f complex is disturbed, even in the absence of high ΔpH (Figure S2).

Starch and sugar metabolism are affected in abc1k1/pgr6

To determine whether the absence of starch granules observed in *abc1k1/pgr6* chloroplasts (Figure 1f,g) was caused by the reduction of photosynthetic activity, starch content was first determined in total rosettes. Starch levels in *abc1k1/pgr6* were reduced compared with the WT, even under moderate light conditions. After a short (32–h) HL treatment starch accumulated in the WT, whereas a reduction in its content was observed in *abc1k1/pgr6* (Figure 3a).

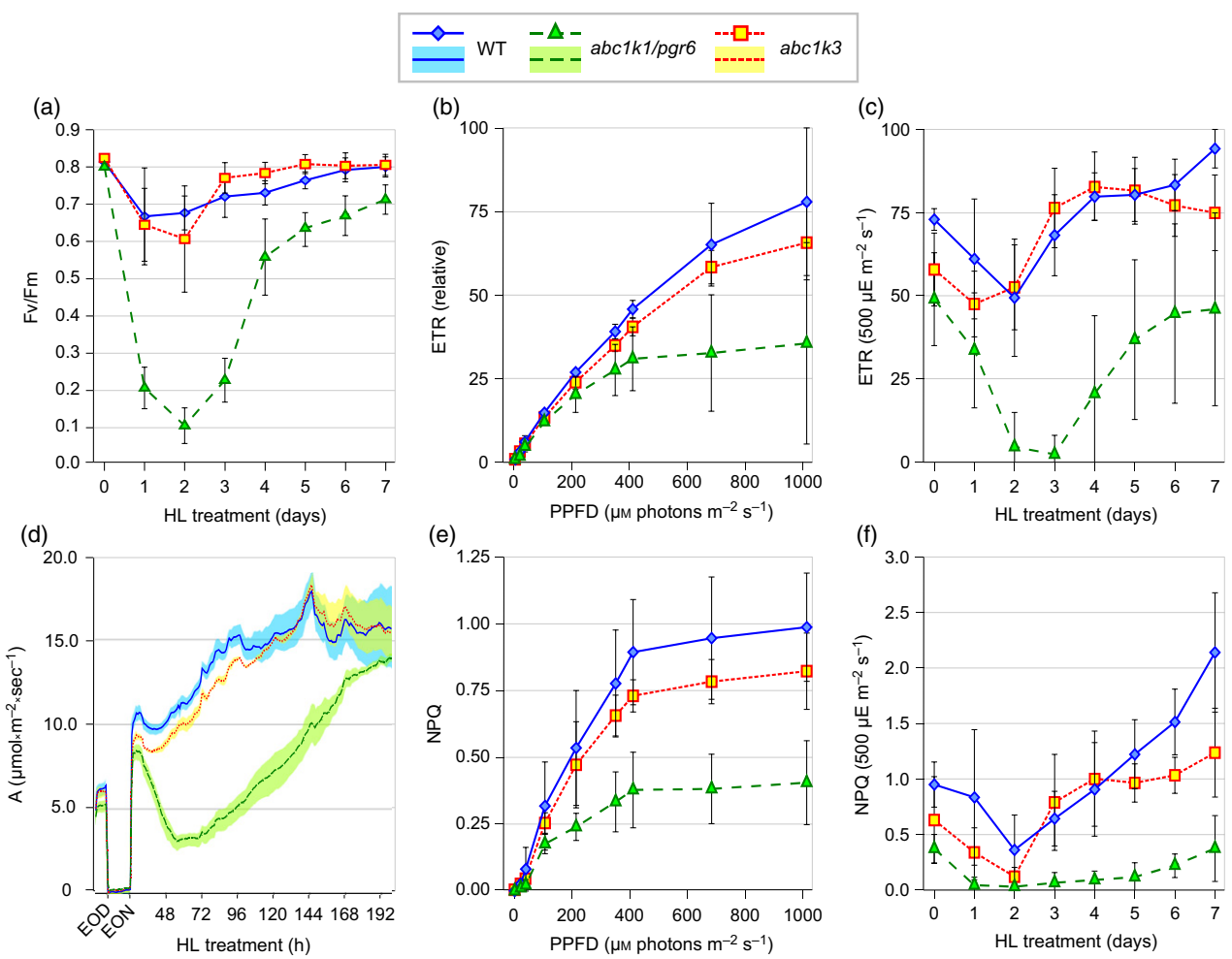

Figure 2. Photosynthetic parameters of the *abc1k1/pgr6* mutant.
(a) Photosystem II (PSII) activity (F_v/F_m) under continuous high light (HL) treatment.
(b, e) Light dependance of electron transport rate (ETR) and non-photochemical quenching (NPQ) in plants grown under moderate light conditions, respectively.
(c, f) ETR and NPQ variations in response to continuous HL treatment, respectively. Leaves (n = 5) from plants exposed to moderate (150 µE m^{-2} sec^{-1}) or high (500 µE m^{-2} sec^{-1}) light intensity were analyzed at intervals of 24 h.
(d) Photosynthetic gas exchange measurement. CO_2 assimilation was measured in three separate chambers for each plant line and the photosynthetic rate was calculated based on the interpolated leaf area (per hour), to avoid fluctuations. Surfaces correspond to SE; EOD, end of day; EON, end of night.

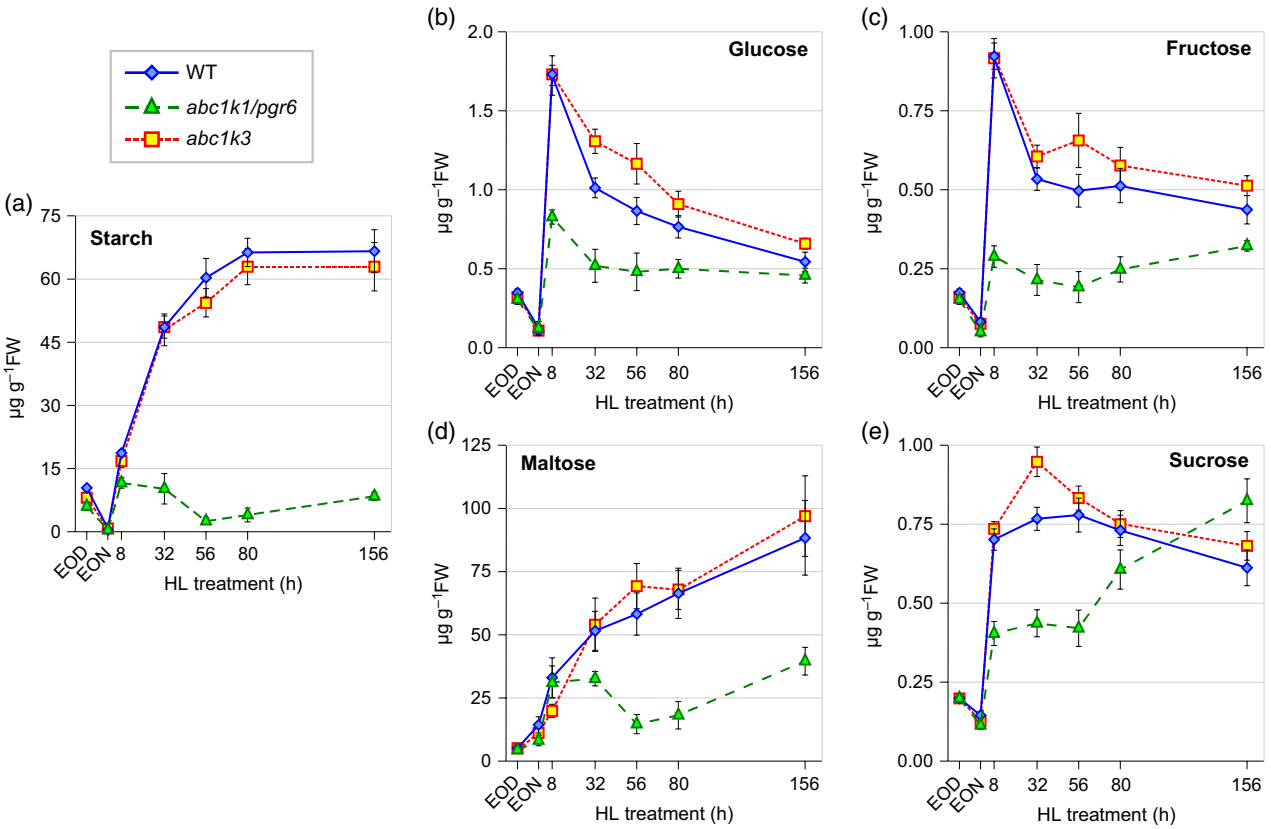

Figure 3. Sugar analysis of plants exposed to high light (HL) treatment: (a) starch; (b) glucose; (c) fructose; (d) maltose; (e) sucrose. Plants were exposed to continuous high light (HL; 500 µE m^{-2} sec^{-1}), and samples were collected at the indicated intervals. Data are from three biological replicates (±SE); EOD, end of day; EON, end of night.

After 7 days of HL treatment, starch accumulation in *abc1k1/pgr6* recovered only partially and in a delayed fashion (Figure 3a), in contrast to the strong recovery in PSII efficiency and CO_2 assimilation rate observed in the same plants (Figure 2a,d, respectively). No significant differences between the *abc1k3* single mutant and WT plants were observed in starch levels (Figure 3a).

The effect on partitioning between starch and free sugars was investigated (Figure 3b–e). Glucose, fructose and maltose levels in *abc1k1/pgr6* leaves were lower than in the WT after a short HL exposure, but recovered after a prolonged HL treatment (Figure 3b–d). Remarkably, the sucrose content in *abc1k1/pgr6* was maximal at about half the level of the WT after a short (56–h) HL treatment, but then accumulated to 1.5-fold the level in the WT after prolonged (156 h) exposure to continuous HL (Figure 3e). Conversely, the *abc1k3* single mutant was similar to the WT, but for a slight accumulation of all the detected sugars after a short HL treatment, in contrast with the *abc1k1/pgr6* mutant (Figure 3b–d).

ABC1K1 affects membrane prenylquinone and carotenoid composition

ABC1-like kinases are known to be implicated in prenylquinone metabolism in mitochondria and chloroplasts. To investigate whether the *abc1k1/pgr6* single mutant has altered prenylquinone and carotenoid contents, lipids of total rosette leaves were rapidly extracted and profiled by ultra-high pressure liquid chromatography coupled with atmospheric pressure chemical ionization-quadrupole time-of-flight mass spectrometry (UHPLC-APCI-QTOFMS). To highlight differences between WT and *abc1k1/pgr6* after HL treatment, untargeted principal component analysis (PCA) was used. Identified prenylquinones and carotenoids are presented in Table S1. Under moderate light conditions WT and *abc1k1/pgr6* samples clustered separately (Figure 4a), and the separation between them strongly increased from day 1 to day 7 of HL exposure (Figure 4b–d). PCA loadings were then investigated to identify compounds responsible for the discrimination between WT and *abc1k1/pgr6*. Under moderate light conditions as well as short HL treatment, higher levels of tocopherols (α-, γ- and δ–T), plastoquinone (PQ–9), plastochromanol (PC–8) and of the xanthophyll lutein were present in WT samples. In contrast, *abc1k1/pgr6* clustered with two oxidized derivates of PQ–9 and PC–8 (PQ-OH and PC-OH), respectively. After 7 days of continuous HL treatment, compared with the WT, *abc1k1/pgr6* accumulated higher levels of α–tocopherol quinone (α-TQ) derived from α–T by

spontaneous oxidation at the thylakoid membranes, the recycling of which depends on VTE1. However, the other tocopherols were significantly increased in WT over *abc1k1/pgr6* (Figure 4d). Interestingly, *abc1k1/pgr6* also coincided with an increased lutein level after 7 days of HL treatment (Figure 4d).

The abundances of other molecules were altered in *abc1k1/pgr6*, but identification was not possible based exclusively on their *m/z* ratio without the use of the correct molecular standards. All detected peaks are listed in Table S2.

The identified prenylquinones and carotenoids were quantified to determine variations between WT and *abc1k1/pgr6* caused by HL exposure (Figure 5a–h). α-, γ- and δ–T levels were similar in WT and *abc1k1/pgr6* under moderate light conditions, but unlike the WT their

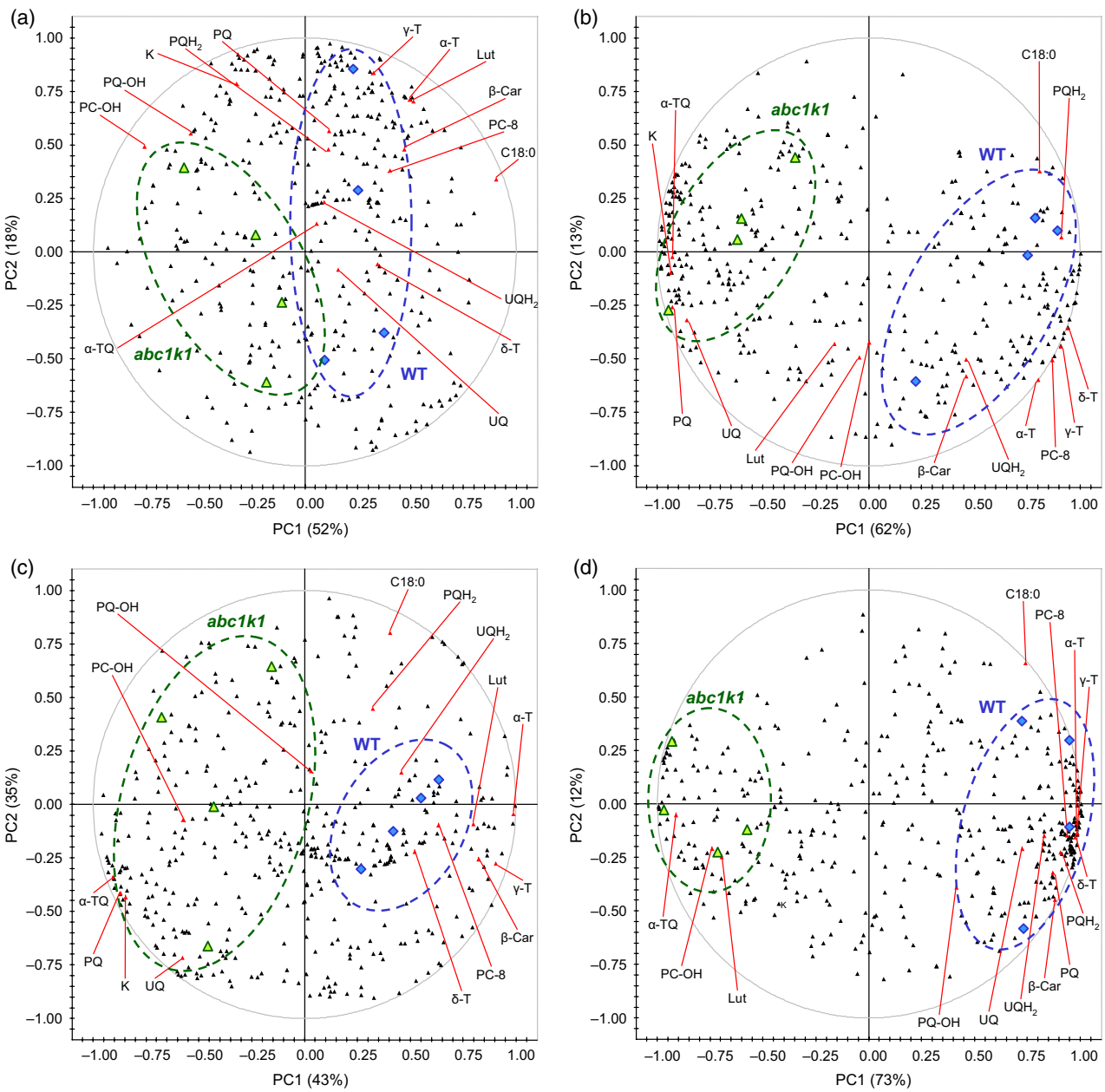

Figure 4. Bi-plots derived from an untargeted principal component analysis (PCA), showing differences between lipid profiles of different plant lines and after HL treatment.
(a) Plants grown under moderate light conditions (150 μE m^{-2} sec^{-1}).
(b–d) Plants exposed to continuous high light (500 μE m^{-2} sec^{-1}) for 1, 2 and 7 days, respectively. Colored symbols correspond to the observations (n = 4 for each plant line) and black triangles represent the variables. PC1 and PC2 are first and second principal components, respectively, with their percentage of explained variance. The identified prenylquinones and carotenoids are indicated (see Table S1). For abbreviations, see main text.

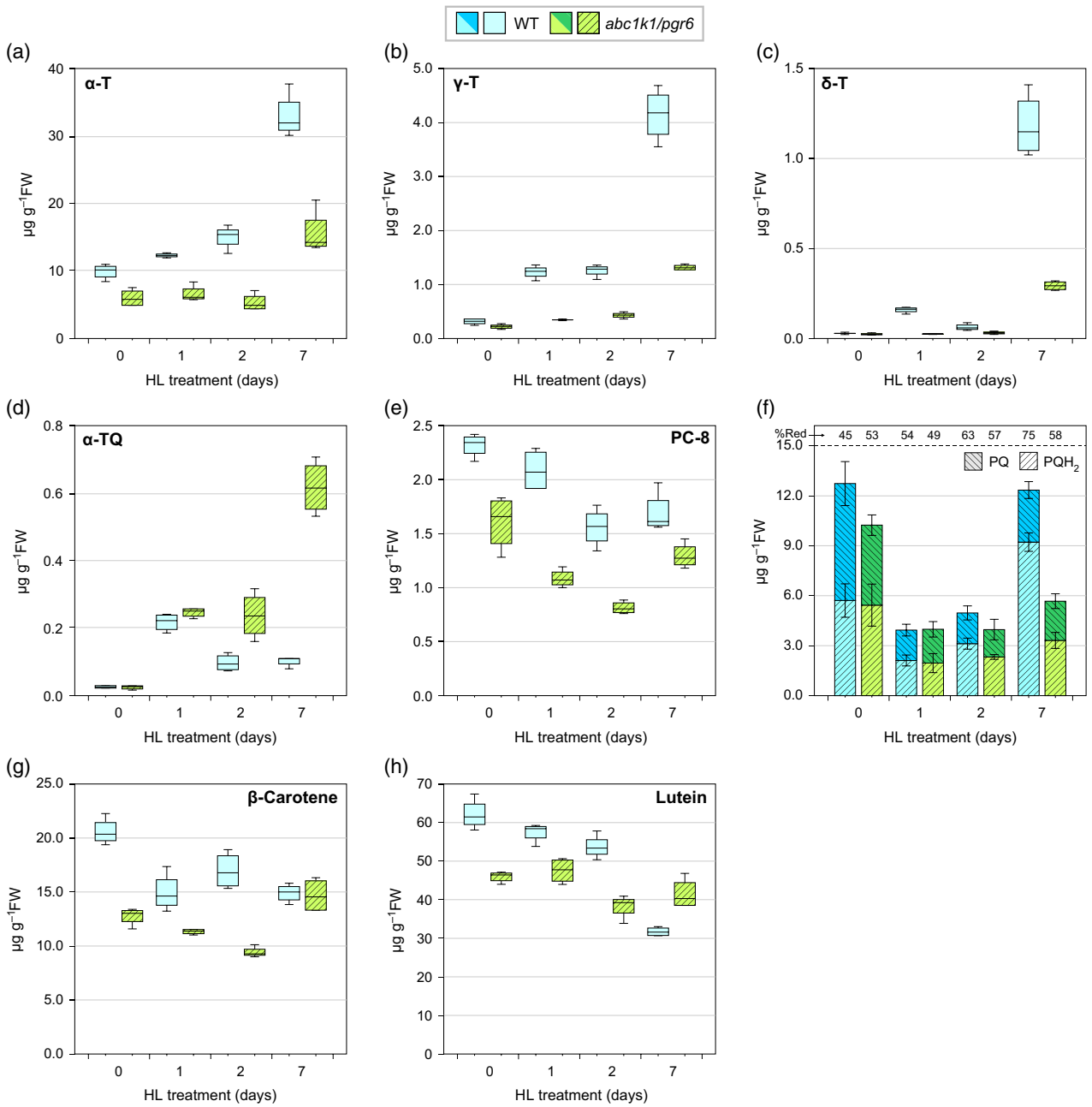

Figure 5. Comparison of the prenylquinone and carotenoid total leaf content: (a) α–tocopherol; (b) γ–tocopherol; (c) δ–tocopherol; (d) α–tocopherol quinone; (e) plastochromanol–8; (f) plastoquinone–9, oxidized (PQ) and reduced (PQH_2) forms (the reduction rate, PQH_2/total PQ–9, is indicated); (g) β–carotene; (h) lutein. Plants grown under moderate light conditions (day 0, 150 µE m^{-2} sec^{-1}) were exposed to continuous high light (500 µE m^{-2} sec^{-1}) for 1, 2 and 7 days, respectively. Data are from four biological replicates (±SD).

content did not increase greatly in *abc1k1/pgr6* under HL treatment (Figure 5a–c). A significantly higher accumulation of α–TQ was observed in *abc1k1/pgr6* under HL treatment, whereas in the WT α–TQ was presumably recycled to α–T (Figure 5d). Moreover, in *abc1k1/pgr6* the level of the PQ–9-derived VTE1 product, plastochromanol–8 (PC–8), was about half that of WT, both under moderate light conditions and throughout the HL treatment (Figure 5e). The total content of PQ–9 was also significantly lower in *abc1k1/pgr6* than in WT under moderate light conditions, as well as after prolonged HL treatment, whereas PQ–9 levels in both genotypes were similar after short exposure to HL (Figure 5f). Furthermore, the redox state of the PQ–9 pool did not significantly

change in *abc1k1/pgr6* after HL exposure, whereas an increased percentage of the reduced form (PQH_2) was detected in the WT, as previously reported (Szymanska and Kruk, 2010; Martinis *et al.*, 2011). Carotenoid content was affected in *abc1k1/pgr6*. In particular, β–carotene and lutein levels were significantly reduced when compared with the WT under both moderate light conditions and after a short exposure to HL. Strikingly, a significant increase of lutein (about 30% more than in the WT) was observed in *abc1k1/pgr6* after prolonged HL treatment, whereas the β–carotene content recovered to WT levels (Figure 5g,h).

Plastoglobule protein composition is altered in the *abc1k1/pgr6* mutant

Considering the relevance of the enzymatic products of the tocopherol cyclase (VTE1) on the observed perturbations in the prenylquinone composition of *abc1k1/pgr6* (Figures 4a–d and 5a–e) and their photoprotective activity during HL acclimation, a possible alteration in VTE1 concentration and subcellular localization was tested by western blotting. Equivalent protein quantities of chloroplast membrane subfractions (PG; envelopes, ENV; thylakoids, THY) were separated by SDS-PAGE, transferred to nitrocellulose and colored with Amido black (Figure 6a, top panel). The identity of the subfractions were checked by western blotting with antibodies towards the two PG markers FBN1a and FBN2 as well as the envelope and thylakoid markers Toc75 and LHCb2, respectively. To confirm the PG localization of ABC1K1, antibodies raised against the kinase were used (Figure 6a). As expected, ABC1K1 was detectable only in the PG fraction purified from WT plants. VTE1 was detected in WT PGs but not in those of the *abc1k1/pgr6* single mutant, comparable with the mutant lacking the PG kinase ABC1K3 (Martinis *et al.*, 2013). To establish whether VTE1 was affected at the level of gene expression or post-transcriptionally, quantitative RT-PCR was performed on total RNA extracted from fresh WT and *abc1k1/pgr6* leaves. A significant increase (2.5-fold) of *VTE1* transcript was detected in *abc1k1/pgr6* when compared with WT plants (Figure 6b), an observation similar to that for the *abc1k3* single mutant (Martinis *et al.*, 2013). Concerning the other proteins investigated by immunoblotting (Figure 6a), the αFBN1a serum detected two distinct proteins with an apparent molecular mass just above 30 kDa, and likely to be identical with the two fibrillins FBN1a and FBN1b, as previously reported (Giacomelli *et al.*, 2006). Interestingly, the upper band (FBN1a) was not detectable and the lower band (FBN1b) was significantly reduced in *abc1k1/pgr6* PGs when compared with WT plants. Also, the fibrillin FBN2 was much less abundant in *abc1k1/pgr6* PGs than in the WT. Finally, a reduction of chlorophyll binding protein LHCb2 was observed in *abc1k1/pgr6* thylakoids, whereas no apparent difference in the outer envelope marker Toc75 was seen between WT and *abc1k1/pgr6* plants.

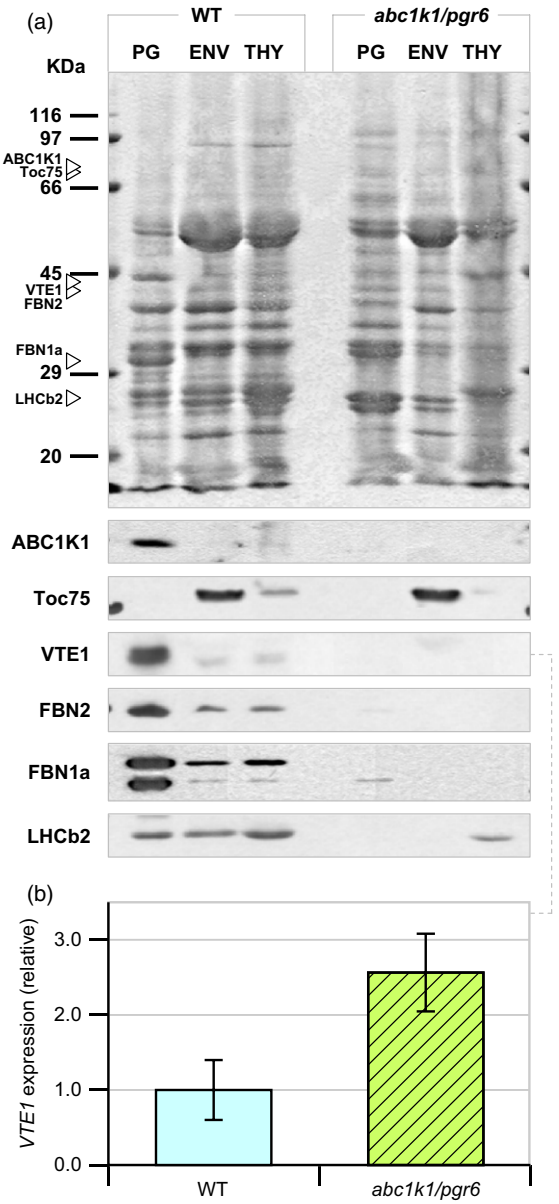

Figure 6. (a) Western blot analysis on purified chloroplast subfractions. Total proteins were extracted from: plastoglobules (PG), envelope (ENV) and thylakoids (THY). Proteins were separated by SDS-PAGE, transferred to nitrocellulose and immunoblotted using the indicated antibodies raised against: the ABC1-like kinase, ABC1K1; the 75–kDa translocon at the outer envelope membrane, Toc75; the tocopherol cyclase, VTE1; the two most abundant plastoglobule fibrillins, FBN1a and FBN2; and the light-harvesting antenna type–II chlorophyll *a*/*b* binding protein, LHCb2. The positions of the detected proteins on the membrane are indicated by white triangles.
(b) Changes in *VTE1* gene expression levels determined by real-time RT-PCR. Total RNA extracted from untreated leaves was used for PCR assays. *ACTIN2* expression levels were used for normalization. Significant differences between samples ($n = 3$ for each plant line) were determined by a one-way ANOVA.

ABC1K1 phosphorylates the tocopherol cyclase

Based on sequence similarities, ABC1K1 is a predicted member of the ABC1/ADCK/UbiB kinase family. Its targets are currently unknown (Vidi *et al.*, 2006; Lundquist *et al.*, 2012b); however, ABC1K1 has been shown to functionally interact with its homolog ABC1K3 (Lundquist *et al.*, 2013), a PG kinase phosphorylating VTE1 *in vitro*, and possibly affecting its recruitment to PGs (Martinis *et al.*, 2013). The quantitative effects of *abc1k1/pgr6* on metabolic products of VTE1 suggest that it is also a target of ABC1K1 kinase. To test this, the mature kinase was produced in a cell-free rabbit reticulocyte lysate and used in kinase assays in the presence or absence of the purified VTE1 and [γ–^{33}P]ATP. The reticulocyte lysate is highly concentrated, containing a large variety of proteins including kinases and their substrates. Therefore, it was used as a negative control in the absence of added substrates and ABC1K1 kinase. In this reaction several weak bands were observed in the background (Figure 7a, IVTmix). In phosphorylation reactions containing both the purified VTE1 and the ABC1K1 *in vitro* product, a significant incorporation of ^{33}P (Figure 7a,b) was detected in a protein band at around 45 kDa that was absent from the control reactions (Figure 7a, IVTmix, ABC1K1 and VTE1). The mass of the phosphoprotein was similar to the predicted mass of VTE1 (43.5 kDa).

In parallel, western blotting was performed using αABC1K1 or αVTE1 antibodies. The 45–kDa phosphoprotein co-migrated with the band detected by αVTE1, strongly supporting that VTE1 was the phosphoprotein (Figure 7c).

DISCUSSION

ABC1K1 affects photosynthetic activity via the modulation of chloroplast lipid metabolism

Recent research showed the mutual stabilization of ABC1K1 and ABC1K3 kinases. In both cases, a reduced level of one kinase was observed in the null mutant of the other kinase. Therefore, the detailed analysis of the single mutants at the time appeared unnecessary (Lundquist *et al.*, 2013). The present work, however, demonstrates that the two mutants have separable phenotypes, suggesting that the reduced kinase levels are sufficient to exert physiological effects.

The results show that the *abc1k1* mutants are allelic to the photosynthetic mutant *pgr6* (Shikanai *et al.*, 1999), and have phenotypes distinct from those of the *abc1k3* mutant (Martinis *et al.*, 2013). This indicates that ABCK1 has specific functions independently of ABC1K3, and that it makes sense to study these by single-mutant analysis. The *abc1k1 abc1k3* double mutant phenotype can be interpreted as a conditional light stress phenotype (Lundquist *et al.*, 2013), but the *pgr6* single mutant phenotype indicates an underlying photosynthetic defect. Based on the increased photoinhibition caused by a short HL treatment and the synergistic phenotype of the *pgr1 pgr6* double mutant in electron transport (Figure S2), it is likely that Cyt b_6f activity is partly impaired in *pgr6*. But considering the strong evidence for PG localization of ABC1K1, it does not appear likely that the kinase is directly involved in either the assembly of the Cyt b_6f key complex or in regulating its activity and hence the formation of the proton gradient across thylakoid membranes, as is the case in the *pgr1* mutant (Munekage *et al.*, 2001; Jahns *et al.*, 2002). For these reasons, the effects on cyt b_6f activity are probably of indirect nature in *abc1k1/pgr6*.

In support of an indirect mode of action, the *abc1k1/pgr6* mutation affects the cellular content of molecules belonging to carotenoid and prenylquinone classes that are known to be involved either in the photosynthesis or in the photoprotection of thylakoid membranes (Figures 4 and 5). PQ–9 levels strongly decreased after 1 and 2 days of HL treatment and then recovered to the initial levels in the WT, but remained low in *abc1k1/pgr6*. The reasons for this are unclear, but we speculate may be a consequence of destructive oxidation under photoinhibitory conditions. The much smaller pool of the electron carrier PQ–9 could limit to some extent to the lower ETR in the *abc1k1/pgr6* mutant after prolonged HL treatment. Also, the distribution of PQ–9 between the photoactive and photoinactive pools in *abc1k1/pgr6* has not been studied so far, but may have an effect on ETR. Lower electron flow rates and the diminished availability of the reduced form of PQ–9 at cyt b_6f potentially explain the *pgr* phenotype, and consequently the reduced induction of NPQ after prolonged HL exposure. Moreover, alterations in PQ–9 levels have previously been associated with severe defects in chloroplast development and chlorophyll accumulation (Motohashi *et al.*, 2003). Under moderate light conditions as well as short exposure to HL intensity, *abc1k1/pgr6* plants had β–carotene and lutein levels lower than WT (Figure 5g,h). Carotenoids have essential roles in protecting photosystems from oxidative damage (Ramel *et al.*, 2012). Defects in the regulation of carotenoid metabolism may therefore also contribute to photoinhibition as well as reduced NPQ. Although zeaxanthin is mainly responsible for the energy-dependent component of NPQ (qE), lutein contributes to the residual qE in *Arabidopsis thaliana* (Muller *et al.*, 2001; Niyogi *et al.*, 2001). Plants lacking zeaxanthin accumulate lutein instead, which partially restores NPQ (Li *et al.*, 2009). The observed increase in lutein and β–carotene levels in the *abc1k1/pgr6* mutant may therefore reflect an adaptive strategy to acclimate to HL intensity. Besides, lutein binds to the L1 site of all Lhc proteins, the occupancy of which is indispensable for protein folding and to successfully quench the chlorophyll triplet state (Dall'Osto *et al.*, 2006). As a consequence, an initial reduction in lutein content in *abc1k1/pgr6* would also explain the observed reduction in

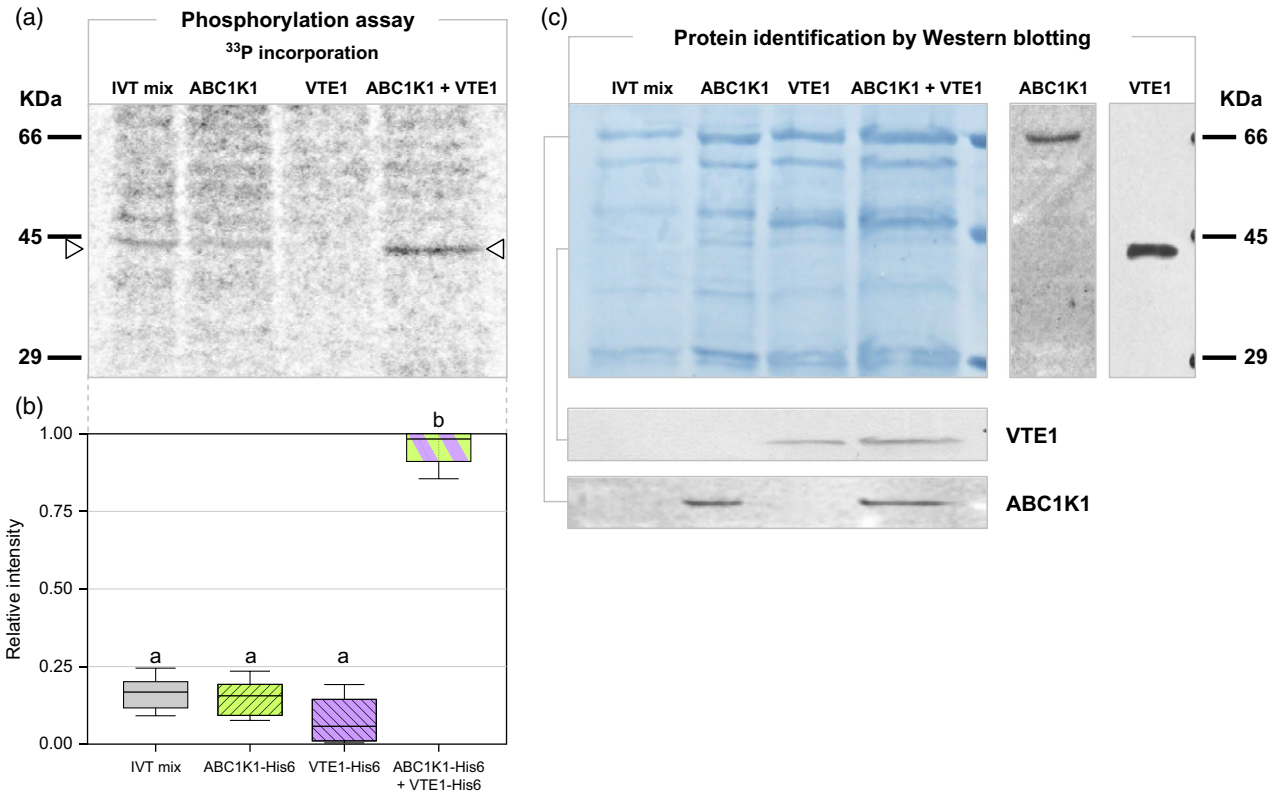

Figure 7. *In vitro* phosphorylation assays.
(a) *In vitro* VTE1 phosphorylation assay by the recombinant ABC1K1. The recombinant kinase was synthesized in rabbit reticulocyte lysate (IVT mix) and used for *in vitro* phosphorylation reactions in the absence or presence of the purified recombinant VTE1-His_6. Because the IVT mix already contains multiple kinases and their phosphorylation targets, a number of faint background bands can be observed in the lysate alone (negative control). Reactions were then supplemented with [γ-^{33}P]ATP, and ^{33}P incorporation in the samples was determined by autoradiography.
(b) Phosphor Imager quantification of the relative intensity at the position of the white arrow (corresponding to VTE1-His_6). Significant differences between samples (n = 4 biological replicates) were determined by a one-way ANOVA.
(c) Independent determination of the positions of ABC1K1-His_6 and VTE1-His_6 on the gel by immunoblotting of separate SDS-PAGE gels. In order to validate the presence of the two proteins in the samples, phosphorylation reactions not supplemented with [γ-^{33}P]ATP were analyzed on separate SDS-PAGE gels, transferred on nitrocellulose and stained with Coomassie Blue (top-left panel). The apparent molecular weight and the presence of ABC1K1-His_6 and VTE1-His_6 in the samples were then determined by immunoblotting (right and lower panels, respectively).

the numbers of chlorophyll-binding proteins of the photosynthetic complexes previously reported (Yang *et al.*, 2012; Lundquist *et al.*, 2013). At the same time, *ABC1K1* is highly predicted to co-express with the ζ–carotene desaturase (ZDS; Figure S3A–C), a key enzyme in both α- and β–carotene biosynthetic pathways that accumulates in PGs during conversion from chloroplast to chromoplast (Ytterberg *et al.*, 2006), and requires PQ–9 as an electron acceptor (Mayer *et al.*, 1992; Norris *et al.*, 1995; Carol and Kuntz, 2001). Plants lacking ZDS are also characterized by a two-fold reduction in chlorophyll content, together with a downregulation in the expression of Lhc components, a lower maximum PSII efficiency and defects in chloroplast development (Dong *et al.*, 2007), similarly to *abc1k1/pgr6* plants.

Unusually, in contrast to the *pgr1* mutant (Munekage *et al.*, 2001), *abc1k1/pgr6* recovered from rapid, HL-induced photoinhibition, and both the F_v/F_m and CO_2 fixation rate were near normal levels after several days of HL treatment. Notably, chlorophyll and Lhc levels as well as leaf thickness were drastically reduced in *abc1k1/pgr6* plants acclimating to HL (Figures 1d–e and 7a), suggesting an acclimation strategy based on absorbing less light energy (Neidhardt *et al.*, 1998; Melis, 2004). Moreover, the substantial differences in the levels of carotenoids observed between WT and *abc1k1/pgr6* plants after the acclimation to HL strongly suggest a possible involvement of carotenoid metabolism. It has previously been observed that *npq1 lut2* double mutants, lacking both zeaxanthin and lutein, and characterized by low NPQ, were able to acclimate to moderately HL intensities (Niyogi *et al.*, 2001). Moreover, the defect in carotenoid metabolism in these plants resulted in lower chlorophyll levels and visible photooxidative damage in the older leaves after prolonged HL treatment, whereas younger ones were relatively unaffected, similar to what was observed in the *abc1k1/pgr6* mutant.

Starch and sugar metabolism are affected in the *abc1k1/pgr6* mutant

Striking alterations in starch and sugar metabolism were observed in the *abc1k1/pgr6* mutant after short (2 days) and prolonged (7 days) exposure to HL intensity (Figure 3a). Reduced starch accumulation in *abc1k1/pgr6* after short HL exposure can be explained by photoinhibition of PSII and a reduced ETR that lead to lower photosynthetic rates (Sharkey *et al.*, 1985). Even under moderate light conditions the *abc1k1/pgr6* mutant had a slightly lower CO_2 assimilation rate (Figure 2d), whereas the photosynthetic efficiency is similar to the WT or is only mildly affected (Figure 2b,e). This is consistent with the slightly lower starch content under moderate light conditions. During HL treatment, *abc1k1/pgr6* plants assimilated significantly less carbon but approached WT rates over time. This might not be sufficient for the maintenance of normal carbon metabolism, resulting in the reduction of starch accumulation and the channeling of assimilated carbon into sugars.

Nevertheless, and despite the recovery in CO_2 assimilation rate after prolonged HL treatment, starch levels did not significantly increase in *abc1k1/pgr6*. However, a significant increase in sucrose accumulation was detected in *abc1k1/pgr6* plants after prolonged HL treatment when compared with the WT (Figure 3e). This suggests that ABC1K1 plays a role in modulating the sucrose:starch ratio. Interestingly, three fructose-bisphosphate aldolase (FBPA) homologs, although not exclusively localized in PGs (Lundquist *et al.*, 2012b), have been previously reported to significantly contribute to the PG proteome (Ytterberg *et al.*, 2006). It has been demonstrated that changes in the levels of the chloroplast FBPAs affect the carbon flux through the Calvin cycle, thus influencing carbon fixation rate and plant growth independently of the levels of Calvin cycle enzymes (Haake *et al.*, 1998, 1999; Uematsu *et al.*, 2012). As a consequence, a possible variation in FBPA activity in the *abc1k1/pgr6* mutant would contribute to explain the observed shift in the carbon allocation towards sucrose synthesis. Consistent with this hypothesis, no significant differences in the abundance of the enzymes involved in the Calvin cycle were observed during similar HL treatments in the *abc1k1 abck3* double mutant when compared with the WT (Lundquist *et al.*, 2013). Moreover, genome-wide gene co-expression analysis showed that *ABC1K1* tightly co-expresses with the sucrose phosphate synthase SPS4F (Figure S3A–C), another key enzyme in the modulation of sucrose synthesis (Strand *et al.*, 2000), the overexpression of which in *A. thaliana* resulted in an increase in the sucrose : starch ratio in leaves (Signora *et al.*, 1998).

Indirect effect of primary metabolism on anthocyanin content

Besides the defect in chlorophyll accumulation, *abc1k1/pgr6* plants were characterized by a significant delay in anthocyanin synthesis under HL treatment (Figure 1b,c). Anthocyanin synthesis modulation in response to changes in light quality and intensity is tightly controlled in higher plants. Apart from direct light sensing through photoreceptors, such as phytochrome and cryptochrome, plants use other mechanisms to integrate this information. Sugars are common regulators of several genes involved in photosynthesis and carbohydrate metabolism, as well as anthocyanin biosynthesis (Rolland *et al.*, 2006; Solfanelli *et al.*, 2006; Das *et al.*, 2011). In particular, it has been demonstrated in *A. thaliana* that high sucrose levels induce anthocyanin synthesis, and that light sensing alone is not sufficient to trigger this adaptation if sucrose is absent (Jeong *et al.*, 2010). The partial recovery of anthocyanin accumulation observed in *abc1k1/pgr6* plants after prolonged HL treatment could then be explained by the significant increase in leaf sucrose content detected after 3 days of HL treatment (Figure 3e). Moreover, it has also been suggested that the redox state of the PQ–9 pool could play a role in sensing variations of the photosynthetic apparatus, being involved in the modulation of anthocyanin synthesis, together with sugar and light signaling (Jeong *et al.*, 2010; Das *et al.*, 2011).

ABC1K1 phosphorylates the tocopherol cyclase, possibly regulating its stability

Chloroplast ABC1-like kinases have been suggested to function in prenylquinone metabolism, because of their similarity to bacterial, yeast and human proteins that have been implicated in ubiquinone metabolism. However, the chloroplast members of this atypical kinase family are characterized by unconventional ATP-binding sites or catalytic domains (Bayer *et al.*, 2012). It is therefore important to demonstrate their kinase function. We here provide evidence that the mature form of ABC1K1 is an active kinase able to phosphorylate the tocopherol cyclase VTE1 *in vitro* in a cell-free reticulocyte extract (Figure 7a–c). The absence of additional bands phosphorylated by ABC1K1 in the cell-free extract suggests considerable specificity of the kinase for VTE1. *In vivo*, VTE1 content is strongly reduced in *abc1k1/pgr6* (Figure 6a), despite an increase in transcript levels (Figure 6b). This suggests that VTE1 activity is post-transcriptionally downregulated in *abc1k1/pgr6*, in agreement with what was previously observed for ABC1K3, a homolog of ABC1K1 also in PG, and affecting VTE1-dependent metabolism (Martinis *et al.*, 2013). In the *abc1k1 abc1k3* double mutant, however, the levels of VTE1 in PGs were unchanged (Lundquist *et al.*, 2013). Possible explanations may be the different protein detection methods used (western blotting versus mass spectrometry) or the different method used for sample normalization (total protein quantity versus optical density of PG fractions). Finally, different effects of the double mutant when compared with the respective single mutants cannot be

excluded. In this study as well as in Martinis *et al.* (2013), single mutants were analyzed in which VTE1 may be differently affected. Interestingly, it has recently been demonstrated that the two PG kinases physically interact *in vivo*, thus suggesting that they could share common targets (Lundquist *et al.*, 2013). Indeed, VTE1 may be one of these. We hypothesize that phosphorylation by ABC1K1, possibly in cooperation with ABC1K3, is required to stabilize VTE1 at PGs *in vivo*, and that without the kinase VTE1 is destabilized, lowering its concentration in *abc1k1/pgr6* PGs (Figure 6a). As a consequence, lower concentrations of the enzymatic products of the tocopherol cyclase (α-, γ-, δ–T and PC–8) were detected in *abc1k1/pgr6* and the activity of the recently discovered tocopherol redox cycle may also be diminished. This would account for the accumulation of α–TQ, a spontaneous oxidation product of α–T that is regenerated via the activity of the tocopherol cyclase VTE1 (Kobayashi and DellaPenna, 2008; Szymanska and Kruk, 2010). Both tocopherols and PC–8, a PQ–9 chromanol derivative with a structure similar to γ–T, are cited for their antioxidant activity and their role together with xanthophylls in preventing PSII photoinhibition and protecting thylakoid membrane lipids from peroxidation (Havaux *et al.*, 2005; Maeda and DellaPenna, 2007; Zbierzak *et al.*, 2010). The defect in tocopherol accumulation under prolonged HL treatment, together with reduced α–TQ recycling, would then further explain the rapid PSII photoinhibition after short HL stress, as well as the higher degree of photooxidative damage observed in *abc1k1/pgr6* plants exposed for several days to continuous HL.

EXPERIMENTAL PROCEDURES

Chemicals

Solvents for plant lipid profiling were tetrahydrofuran (THF, analytical grade, Normapur; VWR, http://be.vwr.com) and ethylacetate (EtAc, analytical grade; Acros Organics, http://www.acros.com). ULC/MS-grade MeOH and water from Biosolve (http://www.biosolve-chemicals.com) were used for the UHPLC-APCI-QTOFMS analyses. Unless indicated, all other chemicals were obtained from Sigma-Aldrich (http://www.sigmaaldrich.com).

Purified standards for lipidomics

The α– and γ–tocopherol (α–T and γ–T, respectively) and phylloquinone (K) standards of HPLC grade (≥99.5%) were obtained from Sigma-Aldrich. The δ–tocopherol (δ–T) standard was from Supelco (now Sigma-Aldrich). The α–TQ, PQ–9 and PC–8 standards were kind gifts from Dr Jerzy Kruk (Jagiellonian University, Kraków, Poland). The oxidized and reduced PQ–9 standards were prepared as reported in Suhara *et al.* (2005), with slight modifications (Martinis *et al.*, 2011). Lutein (Lut) and β–carotene (β–Car) standards were obtained from Extrasynthese (http://www.extrasynthese.com).

Plant material and treatments

Wild type (WT) always refers to *A. thaliana* (L.) Heynh. var. Columbia 0. *pgr6–1* was obtained by ethyl methanesulfonate mutagenesis of *A. thaliana* Columbia *gl1* plants, and is characterized by a single point mutation in the second exon of the gene (5′–ATTGTTTG**G**ACT-3′ mutated to 5′–ATTGTTTG**A**ACT–3′), which generates a stop codon. In addition, *ABC1K1* disruption was analyzed in three T–DNA insertion lines (SALK_109079, SALK_068628 and SALK_057147) from the Nottingham Arabidopsis Stock Centre (NASC, http://arabidopsis.info; Alonso *et al.*, 2003). Homozygous plants were selected by PCR genotyping (Appendix S1; Figure S1A–D). The visual phenotype, protein patterns, photosynthetic parameters and lipid composition of the mutants were identical (Figure S1E–G). Therefore, only *abc1k1–2* was used for further experimentation. The absence of ABC1K1 in western blot analysis confirmed that *abc1k1–2* is a null allele (Figure 6a).

Plants were grown on soil under standard growth conditions (150 μE m^{-2} sec^{-1}, 8–h light/16–h dark, at 21/18°C, with 55% relative air humidity) according to the protocol described in Hiltbrunner *et al.* (2001), with slight modifications (Martinis *et al.*, 2013). In particular, HL treatment was carried out with 1- or 2–month-old rosettes under continuous HL (500 μE m^{-2} sec^{-1}, 21°C and 55% relative air humidity). Higher light intensities were avoided to rule out the appearance of pleiotropic phenotypes caused by the rapid induction of cellular damage.

Determination of the photosynthetic parameters

Maximum quantum efficiency of photosystem II (F_v/F_m), ETR and non-photochemical quenching (NPQ) were fluorometrically determined using a MINI-PAM Photosynthesis Yield Analyzer (Walz, http://www.walz.com).

Photosynthetic gas exchange was measured using a custom-built multichamber system connected in parallel with an infrared gas analyzer (Licor7000; LI–COR, http://www.licor.com). Arabidopsis plants were grown under short-day conditions until both genotypes reached the same developmental stage, then gas exchange was measured for 7 days. After the first 24 h, growth conditions were switched to continuous HL. During the measurement, air with a CO_2 content pf 736 mgm^{-3} and a relative humidity of 65% was channeled through the system at a flow rate of 200 μmol sec^{-1}. Each chamber was measured consecutively for 6 min, and the average value was taken for the light and the dark periods. At the end of the light period, a picture was taken to calculate the projected leaf area for each plant. Based on the projected leaf area, photosynthetic and respiration rates were calculated with the ΔCO_2 and ΔH_2O values gained from the gas exchange system.

Analysis of starch and sugar metabolism

For the measurement of starch in total rosettes, the perchloric acid extraction method described by Delatte *et al.* (2006) was used, with slight modifications. Briefly, samples comprising entire individual rosettes were frozen in Eppendorf tubes and pulverized while still frozen using a Mixer Mill (Retsch, http://www.retsch.com). The frozen powder was extracted in 800 μl of ice-cold 1 M perchloric acid for 5 min with intermittent mixing. All the subsequent steps were carried out between 0 and 4°C. After centrifugation (3000 ***g*** for 10 min at 4°C), the insoluble material in the pellet was washed once with water and three times with 80% (v/v) ethanol. Starch content in the insoluble material was then measured by determining the glucose released by treatment with α–amylase and amyloglucosidase, as described by Smith and Zeeman (2006). Briefly, starch granules were extracted in EtOH to remove free glucose, solubilized by heating, and digested to glucose with a preparation of α–amyloglucosidase and α–amylase. Glucose content was then enzymatically assayed using hexokinase and glucose

6–phosphate dehydrogenase to convert glucose to 6–phosphogluconate, with a concomitant reduction of NAD to NADH (Kunst *et al.*, 1988).

For the measurement of sugars, the same perchloric acid extraction method was used. After centrifugation, the supernatant (soluble fraction) was adjusted to pH 5 by adding 2 M KOH and 0.4 M 2–(*N*–morpholine)-ethanesulphonic acid (MES). Precipitated potassium perchlorate was removed by centrifugation (2000 ***g*** for 15 min at 4°C), and sugars (glucose, fructose, sucrose and maltose) in the supernatant were measured using HPAEC-PAD, as described in Fulton *et al.* (2008), with minor modifications. Samples of the neutralized soluble fraction (100 ml) were applied to sequential 1.5–ml columns of Dowex-50-Hydrogen (acidic) and Dowex-1-Chloride (basic) (Sigma-Aldrich). The neutral compounds were eluted with 4 ml of water, lyophilized and redissolved in 100 ml of water. The sugars were separated on a Dionex PA–20 column according to the following conditions: eluent A, 100 mM NaOH; eluent B, 150 mM NaOH and 500 mM sodium acetate. The gradients were as follows: 0.0–7.0 min, 100% A; 7.1–26.5 min, a concave gradient to 20% A and 80% B (elution of sugars); 26.6–32.0 min, 20% A and 80% B (column wash step); 32.1–40.0 min, 100% A (column re-equilibration). Peaks were identified by co-elution with known sugar standards. Peak areas were determined using the CHROMELEON software (Dionex, http://www.dionex.com).

Arabidopsis membrane prenylquinone profiling

Liquid chromatography–mass spectrometry analyses of leaf extracts were performed as described in Martinis *et al.* (2011), with slight modifications allowing the simultaneous separation and detection of prenylquinones and carotenoids in the range between 235 and 1200 Da (Martinis *et al.*, 2013).

Preparation of αABC1K1 polyclonal antibodies

The coding sequence of ABC1K1 was subcloned by Gateway® LR recombination in p0GWA, a derivate of pET22d (Merck, http://www.merck.com), described in Busso *et al.* (2005), and encoding for a C–terminal His_6 tag. The full-length His_6-tagged precursor protein was then expressed in *Escherichia coli* BL21 (DE3) cells (Novagen, now EMD Millipore, http://www.emdmillipore.com), purified under denaturing conditions by Ni-NTA affinity chromatography (Qiagen, http://www.qiagen.com), according to the supplier's recommendations, and then used to produce rabbit polyclonal antibodies (Eurogentec, http://www.eurogentec.com). αABC1K1 antibodies were then purified from serum by affinity chromatography, using the recombinant ABC1K1-His_6 coupled to Affi-Gel 15 (Bio-Rad, http://www.bio-rad.com) as stationary phase, according to the manufacturer's instructions.

Chloroplast fractionation and protein analysis

Chloroplast membranes were prepared and fractionated as described by Vidi *et al.* (2006), with slight modifications. To prevent proteolysis, 0.5% (v/v) protease inhibitor cocktail for plant cell extracts (P9599; Sigma-Aldrich) was added. To inhibit dephosphorylation, 1% (v/v) phosphatase inhibitor cocktail 2 (P5726; Sigma-Aldrich) was included. Total proteins were precipitated by chloroform-methanol (Wessel and Flugge, 1984), dissolved in an appropriate volume of SDS-PAGE sample buffer [50 mM Tris/HCl, pH 6.8, 0.1 M DTT, 2% (w/v) SDS, 0.1% (w/v) bromophenol blue, 10% (v/v) glycerol], and separated by SDS-PAGE. After transfer to nitrocellulose, the blots were probed with sera raised against ABC1K1 (this paper), the Toc75 outer membrane marker (Hiltbrunner *et al.*, 2001), the light-harvesting antenna type–II chlorophyll *a*/*b* binding protein (LHCb2, a kind gift from Dr K. Apel, Cornell University, Ithaca, NY, USA), the tocopherol cyclase (VTE1; Kanwischer *et al.*, 2005), and the two fibrillins FBN1a and FBN2 (Vidi *et al.*, 2006).

Phosphorylation assays

In order to test VTE1 as a possible target of ABC1K1, the coding sequence for the kinase was cloned in the previously decribed p0GWA expression vector, removing the predicted chloroplast transit peptide (prediction by TARGETP 1.1; Emanuelsson *et al.*, 2007). The mature ABC1K1 was produced *in vitro* using the TNT® Quick Coupled Transcription/Translation System (Promega, http://www.promega.com), following the manufacturer's recommendations. The expression vector VTE1-pQE31, coding the mature VTE1 (no transit peptide), was kindly provided by Dr P. Dörmann (University of Bonn, Germany). Protein expression and purification were carried out as previously described (Porfirova *et al.*, 2002; Martinis *et al.*, 2013). *In vitro* phosphorylation reactions were performed as previously described (Martinis *et al.*, 2013). The nature of the radioactive phosphoprotein was confirmed in a parallel western blot using antibodies against VTE1 (see section Chloroplast fractionation and protein analysis).

Gene expression

Total RNA were purified from *A. thaliana* leaves using the RNeasy Plant Mini Kit (Qiagen), following the supplier's protocol. DNase treatment was performed on column using the RNase-free DNase set (Qiagen). cDNAs were prepared by the GoScript™ Reverse Transcriptase kit (Promega) in the presence of RNasin RNase inhibitors (Promega), and stored at −20°C. For the analysis of *VTE1* expression, quantitative PCR reactions ($n = 3$) were performed using the primers previously described (Martinis *et al.*, 2013), using the ABsolute™ qPCR SYBR® Green mix (ABgene, Epsom, UK (http://www.thermoscientificbio.com/abgene/)). SYBR® Green emission was detected in real-time in an iQ5 Optical System (Bio-Rad) and data were analyzed with the included software. A one-way analysis of variance (ANOVA) was performed on the data obtained. In the case of significant differences, Tukey's honestly significant difference (HSD) test was applied at a significance level of $P < 0.05$ to separate the means. Gene co-expression was determined *in silico* using the ATTED-II 6.0 database (Obayashi *et al.*, 2011).

Chlorophyll quantification

Leaves ($n = 3$) were exactly weighted and extracted in 80% acetone. Total chlorophyll levels were then spectrophotometrically determined, as previously described (Wintermans and Demots, 1965).

Chloroplast ultrastructure analysis

Ultrathin leaf sections for electron microscopy analysis were prepared as previously described (Martinis *et al.*, 2013).

Accession Numbers

Sequence data are from the EMBL/GenBank data libraries, and have the following accession numbers AEE85904.1 (*ABC1K1*, At4g31390.1), AEE36271.1 (ABC1K3, At1g79600.1), AEE86116.1 (*VTE1*, At4g32770.1), AEE74149.1 (*ZDS*, At3g04870.1), AEC07161.1 (*FBPA1*, At2g21330.1), AEE87003.1 (*FBPA2*, At4g38970.1), AEC05406.1 (*FBPA3*, At2g01140.1), AEE82845.1 (*SPS4F*, At4g10120.1) AEE82363.1 (*FBN1a*, At4g04020.1), AEC09113.1 (*FBN2*, At2g35490.1), AEC05893.1

(*LHCB2*, At2g05070.1), AEE31832.1 (*TOC75*, At1g35860.1) and AEE76147.1 (*ACTIN2*, At3g18780.1).

ACKNOWLEDGEMENTS

We thank Jerzy Kruk from Jagiellonian University for his kind gifts of purified α–TQ, PQ–9 and PC–8 standards, and Claus Wedekind from the University of Lausanne for providing carotenoid standards. GG acknowledges support from the Swiss Plant Science Web. FK was supported by UniNE, SystemsX PGCE, NCCR Plant Survival, SNF 31003A_127380 and SNF 31003A_144156. Kaname Kimura (Nara Institute of Science and Technology) is gratefully acknowledged for his positional cloning of the *PGR6* gene.

SUPPORTING INFORMATION

Additional Supporting Information may be found in the online version of this article.

Figure S1. Isolation of *ABC1K1/PGR6* mutant alleles.

Figure S2. Enhancement of the photosynthetic phenotype in the *pgr1 pgr6* double mutant.

Figure S3. Predicted *ABC1K1* co-expressed gene network.

Table S1. List of the molecules identified from UHPLC-APCI-QTOFMS data acquired in negative ionization mode.

Table S2. List of all the molecular markers detected by UHPLC-APCI-QTOFMS lipid profiling and relative abundance in samples analyzed.

Appendix S1. Genotyping of the *abc1k1/pgr6* mutant.

REFERENCES

Alonso, J.M., Stepanova, A.N., Leisse, T.J. *et al.* (2003) Genome-wide Insertional mutagenesis of *Arabidopsis thaliana*. *Science*, **301**, 653–657.

Bayer, R.G., Stael, S., Rocha, A.G., Mair, A., Vothknecht, U.C. and Teige, M. (2012) Chloroplast-localized protein kinases: a step forward towards a complete inventory. *J. Exp. Bot.* **63**(4), 1713–1723.

Brehelin, C. and Kessler, F. (2008) The plastoglobule: a bag full of lipid biochemistry tricks. *Photochem. Photobiol.* **84**, 1388–1394.

Busso, D., Delagoutte-Busso, B. and Moras, D. (2005) Construction of a set Gateway-based destination vectors for high-throughput cloning and expression screening in *Escherichia coli*. *Anal. Biochem.* **343**, 313–321.

Carol, P. and Kuntz, M. (2001) A plastid terminal oxidase comes to light: implications for carotenoid biosynthesis and chlororespiration. *Trends Plant Sci.* **6**, 31–36.

Dall'Osto, L., Lico, C., Alric, J., Giuliano, G., Havaux, M. and Bassi, R. (2006) Lutein is needed for efficient chlorophyll triplet quenching in the major LHCII antenna complex of higher plants and effective photoprotection *in vivo* under strong light. *BMC Plant Biol.* **27**, 6–32.

Das, P.K., Geul, B., Choi, S.-B., Yoo, S.-D. and Park, Y.-I. (2011) Photosynthesis-dependent anthocyanin pigmentation in *Arabidopsis*. *Plant Signal. Behav.* **6**, 23–25.

Delatte, T., Trevisan, M., Parker, M.L. and Zeeman, S.C. (2006) *Arabidopsis* mutants *Atisa1* and *Atisa2* have identical phenotypes and lack the same multimeric isoamylase, which influences the branch point distribution of amylopectin during starch synthesis. (vol 41, pg 815, 2005). *Plant J.* **45**, 870.

Dong, H.L., Deng, Y., Mu, J.Y., Lu, Q.T., Wang, Y.Q., Xu, Y.Y., Chu, C.C., Chong, K., Lu, C.M. and Zuo, J.R. (2007) The *Arabidopsis Spontaneous Cell Death1* gene, encoding a zeta-carotene desaturase essential for carotenoid biosynthesis, is involved in chloroplast development, photoprotection and retrograde signalling. *Cell Res.* **17**, 458–470.

Emanuelsson, O., Brunak, S., von Heijne, G. and Nielsen, H. (2007) Locating proteins in the cell using TargetP, SignalP and related tools. *Nat. Protoc.* **2**, 953–971.

Fulton, D.C., Stettler, M., Mettler, T. *et al.* (2008) beta-AMYLASE4, a noncatalytic protein required for starch breakdown, acts upstream of three active beta-amylases in *Arabidopsis* chloroplasts. *Plant Cell*, **20**, 1040–1058.

Giacomelli, L., Rudella, A. and van Wijk, K.J. (2006) High light response of the thylakoid proteome in *Arabidopsis* wild type and the ascorbate-deficient mutant *vtc2-2*. A comparative proteomics study. *Plant Physiol.* **141**, 685–701.

Haake, V., Zrenner, R., Sonnewald, U. and Stitt, M. (1998) A moderate decrease of plastid aldolase activity inhibits photosynthesis, alters the levels of sugars and starch, and inhibits growth of potato plants. *Plant J.* **14**, 147–157.

Haake, V., Geiger, M., Walch-Liu, P., Engels, C., Zrenner, R. and Stitt, M. (1999) Changes in aldolase activity in wild type potato plants are important for acclimation to growth irradiance and carbon dioxide concentration, because plastid aldolase exerts control over the ambient rate of photosynthesis across a range of growth conditions. *Plant J.* **17**, 479–489.

Havaux, M., Eymery, F., Porfirova, S., Rey, P. and Dormann, P. (2005) Vitamin E protects against photoinhibition and photooxidative stress in *Arabidopsis thaliana*. *Plant Cell*, **17**, 3451–3469.

Hiltbrunner, A., Bauer, J., Vidi, P.A., Infanger, S., Weibel, P., Hohwy, M. and Kessler, F. (2001) Targeting of an abundant cytosolic form of the protein import receptor at Toc159 to the outer chloroplast membrane. *J. Cell Biol.* **154**, 309–316.

Jahns, P., Graf, M., Munekage, Y. and Shikanai, T. (2002) Single point mutation in the Rieske iron-sulfur subunit of cytochrome b(6)/f leads to an altered pH dependence of plastoquinol oxidation in *Arabidopsis*. *FEBS Lett.* **519**, 99–102.

Jeong, S.W., Das, P.K., Jeoung, S.C. *et al.* (2010) Ethylene suppression of sugar-induced anthocyanin pigmentation in *Arabidopsis*. *Plant Physiol.* **154**, 1514–1531.

Kanwischer, M., Porfirova, S., Bergmuller, E. and Dormann, P. (2005) Alterations in tocopherol cyclase activity in transgenic and mutant plants of *Arabidopsis* affect tocopherol content, tocopherol composition, and oxidative stress. *Plant Physiol.* **137**, 713–723.

Kobayashi, N. and DellaPenna, D. (2008) Tocopherol metabolism, oxidation and recycling under high light stress in *Arabidopsis*. *Plant J.* **55**, 607–618.

Kunst, A., Draeger, B. and Ziegenhorn, J. (1988) UV methods with heksokinase and glucose-6-phosphate dehydrogenase. In *Methods in Enzymatic Analysis*, 3rd edn, Vol. 6 (Bergmeyer, H.U., ed.). Weinheim, Germany: Chemie, pp. 163–171.

Li, Z.R., Ahn, T.K., Avenson, T.J., Ballottari, M., Cruz, J.A., Kramer, D.M., Bassi, R., Fleming, G.R., Keasling, J.D. and Niyogi, K.K. (2009) Lutein accumulation in the absence of zeaxanthin restores nonphotochemical quenching in the *Arabidopsis thaliana npq1* mutant. *Plant Cell*, **21**, 1798–1812.

Lundquist, P.K., Davis, J.I. and van Wijk, K.J. (2012a) ABC1K atypical kinases in plants: filling the organellar kinase void. *Trends Plant Sci.* **17**, 546–555.

Lundquist, P.K., Poliakov, A., Bhuiyan, N.H., Zybailov, B., Sun, Q. and van Wijk, K.J. (2012b) The functional network of the *Arabidopsis* plastoglobule proteome based on quantitative proteomics and genome-wide coexpression analysis. *Plant Physiol.* **158**, 1172–1192.

Lundquist, P.K., Poliakov, A., Giacomelli, L. *et al.* (2013) Loss of plastoglobule kinases ABC1K1 and ABC1K3 causes conditional degreening, modified prenyl-lipids, and recruitment of the jasmonic acid pathway. *Plant Cell*, **25**(5), 1818–1839.

Maeda, H. and DellaPenna, D. (2007) Tocopherol functions in photosynthetic organisms. *Curr. Opin. Plant Biol.* **10**, 260–265.

Martinis, J., Kessler, F. and Glauser, G. (2011) A novel method for prenylquinone profiling in plant tissues by ultra-high pressure liquid chromatography-mass spectrometry. *Plant Methods*, **7**, 23.

Martinis, J., Glauser, G., Valimareanu, S. and Kessler, F. (2013) A chloroplast ABC1-like kinase regulates Vitamin E metabolism in *Arabidopsis thaliana*. *Plant Physiol.* **162**(2), 652–662.

Mayer, M.P., Nievelstein, V. and Beyer, P. (1992) Purification and characterization of a NADPH dependent oxidoreductase from chromoplasts of *Narcissus pseudonarcissus* - a redox-mediator possibly involved in carotene desaturation. *Plant Physiol. Biochem.* **30**, 389–398.

Melis, A. (2004) Excitation energy transfer: functional and dynamic aspects of Ihc (cab) proteins. In *Oxygenic Photosynthesis: The Light Reactions* (Ort, D.R., Yocum, C.F. and Heichel, I.F., eds). Netherlands: Springer, pp. 523–538.

Motohashi, R., Ito, T., Kobayashi, M., Taji, T., Nagata, N., Asami, T., Yoshida, S., Yamaguchi-Shinozaki, K. and Shinozaki, K. (2003) Functional analysis of the 37 kDa inner envelope membrane polypeptide in chloroplast biogenesis using a Ds-tagged *Arabidopsis* pale-green mutant. *Plant J.* **34**, 719–731.

Muller, P., Li, X.P. and Niyogi, K.K. (2001) Non-photochemical quenching. A response to excess light energy. *Plant Physiol.* **125**, 1558–1566.

Munekage, Y., Takeda, S., Endo, T., Jahns, P., Hashimoto, T. and Shikanai, T. (2001) Cytochrome b(6)f mutation specifically affects thermal dissipation of absorbed light energy in *Arabidopsis*. *Plant J.* **28**, 351–359.

Munekage, Y., Hojo, M., Meurer, J., Endo, T., Tasaka, M. and Shikanai, T. (2002) PGR5 is involved in cyclic electron flow around photosystem I and is essential for photoprotection in *Arabidopsis*. *Cell*, **110**, 361–371.

Nakagami, H., Sugiyama, N., Mochida, K., Daudi, A., Yoshida, Y., Toyoda, T., Tomita, M., Ishihama, Y. and Shirasu, K. (2010) Large-scale comparative phosphoproteomics identifies conserved phosphorylation sites in plants. *Plant Physiol.* **153**, 1161–1174.

Neidhardt, J., Benemann, J.R., Zhang, L.P. and Melis, A. (1998) Photosystem-II repair and chloroplast recovery from irradiance stress: relationship between chronic photoinhibition, light-harvesting chlorophyll antenna size and photosynthetic productivity in *Dunaliella salina* (green algae). *Photosynth. Res.* **56**, 175–184.

Niyogi, K.K., Shih, C., Chow, W.S., Pogson, B.J., DellaPenna, D. and Bjorkman, O. (2001) Photoprotection in a zeaxanthin- and lutein-deficient double mutant of *Arabidopsis*. *Photosynth. Res.* **67**, 139–145.

Norris, S.R., Barrette, T.R. and DellaPenna, D. (1995) Genetic dissection of carotenoid synthesis in *Arabidopsis* defines plastoquinone as an essential component of phytoene desaturation. *Plant Cell*, **7**, 2139–2149.

Obayashi, T., Nishida, K., Kasahara, K. and Kinoshita, K. (2011) ATTED-II updates: condition-specific gene coexpression to extend coexpression analyses and applications to a broad range of flowering plants. *Plant Cell Physiol.* **52**, 213–219.

Poon, W.W., Davis, D.E., Ha, H.T., Jonassen, T., Rather, P.N. and Clarke, C.F. (2000) Identification of *Escherichia coli ubiB*, a gene required for the first monooxygenase step in ubiquinone biosynthesis. *J. Bacteriol.* **182**, 5139–5146.

Porfirova, S., Bergmuller, E., Tropf, S., Lemke, R. and Dormann, P. (2002) Isolation of an *Arabidopsis* mutant lacking vitamin E and identification of a cyclase essential for all tocopherol biosynthesis. *Proc. Natl Acad. Sci. USA*, **99**, 12495–12500.

Ramel, F., Birtic, S., Cuiné, S., Triantaphylidès, C., Ravanat, J.-L. and Havaux, M. (2012) Chemical quenching of singlet oxygen by carotenoids in plants. *Plant Physiol.* **158**, 1267–1278.

Rolland, F., Baena-Gonzalez, E. and Sheen, J. (2006) Sugar sensing and signaling in plants: conserved and novel mechanisms. In *Annual Review of Plant Biology*, Vol **57**, Palo Alto: Annual Reviews Inc., pp. 675–709.

Sharkey, T.D., Berry, J.A. and Raschke, K. (1985) Starch and sucrose synthesis in phaseolus-vulgaris as affected by light, CO_2, and abscisic-acid. *Plant Physiol.* **77**, 617–620.

Shikanai, T., Munekage, Y., Shimizu, K., Endo, T. and Hashimoto, T. (1999) Identification and characterization of Arabidopsis mutants with reduced quenching of chlorophyll fluorescence. *Plant Cell Physiol.* **40**, 1134–1142.

Signora, L., Galtier, N., Skot, L., Lucas, H. and Foyer, C.H. (1998) Over-expression of sucrose phosphate synthase in *Arabidopsis thaliana* results in increased foliar sucrose/starch ratios and favours decreased foliar carbohydrate accumulation in plants after prolonged growth with CO_2 enrichment. *J. Exp. Bot.* **49**, 669–680.

Smith, A.M. and Zeeman, S.C. (2006) Quantification of starch in plant tissues. *Nat. Protoc.* **1**, 1342–1345.

Solfanelli, C., Poggi, A., Loreti, E., Alpi, A. and Perata, P. (2006) Sucrose-specific induction of the anthocyanin biosynthetic pathway in *Arabidopsis*. *Plant Physiol.* **140**, 637–646.

Strand, A., Zrenner, R., Trevanion, S., Stitt, M., Gustafsson, P. and Gardestrom, P. (2000) Decreased expression of two key enzymes in the sucrose biosynthesis pathway, cytosolic fructose-1,6-bisphosphatase and sucrose phosphate synthase, has remarkably different consequences for photosynthetic carbon metabolism in transgenic *Arabidopsis thaliana*. *Plant J.* **23**, 759–770.

Suhara, Y., Kamao, M., Tsugawa, N. and Okano, T. (2005) Method for the determination of vitamin K homologues in human plasma using high-performance liquid chromatography-tandem mass spectrometry. *Anal. Chem.* **77**, 757–763.

Szymanska, R. and Kruk, J. (2010) Plastoquinol is the main prenyllipid synthesized during acclimation to high light conditions in *Arabidopsis* and is converted to plastochromanol by tocopherol cyclase. *Plant Cell Physiol.* **51**, 537–545.

Uematsu, K., Suzuki, N., Iwamae, T., Inui, M. and Yukawa, H. (2012) Increased fructose 1,6-bisphosphate aldolase in plastids enhances growth and photosynthesis of tobacco plants. *J. Exp. Bot.* **63**, 3001–3009.

Vidi, P.A., Kanwischer, M., Baginsky, S., Austin, J.R., Csucs, G., Dormann, P., Kessler, F. and Brehelin, C. (2006) Tocopherol cyclase (VTE1) localization and vitamin E accumulation in chloroplast plastoglobule lipoprotein particles. *J. Biol. Chem.* **281**, 11225–11234.

Wessel, D. and Flugge, U.I. (1984) A method for the quantitative recovery of protein in dilute-solution in the presence of detergents and lipids. *Anal. Biochem.* **138**, 141–143.

Wintermans, J.F.G.M. and Demots, A. (1965) Spectrophotometric characteristics of chlorophylls a and b and their pheophytins in ethanol. *Biochim. Biophys. Acta*, **109**, 448.

Xie, L.T.X., Hsieh, E.J., Watanabe, S., Allan, C.M., Chen, J.Y., Tran, U.C. and Clarke, C.F. (2011) Expression of the human atypical kinase ADCK3 rescues coenzyme Q biosynthesis and phosphorylation of Coq polypeptides in yeast *coq8* mutants. *Biochim. Biophys. Acta*, **1811**, 348–360.

Yang, S., Zeng, X., Li, T., Liu, M., Zhang, S., Gao, S., Wang, Y., Peng, C., Li, L. and Yang, C. (2012) AtACDO1, an ABC1-like kinase gene, is involved in chlorophyll degradation and the response to photooxidative stress in *Arabidopsis*. *J. Exp. Bot.* **63**, 3959–3973.

Ytterberg, A.J., Peltier, J.B. and van Wijk, K.J. (2006) Protein profiling of plastoglobules in chloroplasts and chromoplasts. A surprising site for differential accumulation of metabolic enzymes. *Plant Physiol.* **140**, 984–997.

Zbierzak, A.M., Kanwischer, M., Wille, C. *et al.* (2010) Intersection of the tocopherol and plastoquinol metabolic pathways at the plastoglobule. *Biochem. J.* **425**, 389–399.